Available online at www.sciencedirect.com
SCIENCE DIRECT®
Thermochimica Acta 421 (2004) 51–58
thermochimica acta
www.elsevier.com/locate/tca

Decomposition of the synthetic hydrotalcites mountkeithite and honessite—a high resolution thermogravimetric analysis and infrared emission spectroscopic study

Ray L. Frost*, Kristy L. Erickson

Inorganic Materials Research Program, School of Physical and Chemical Sciences, Queensland University of Technology, GPO Box 2434, Brisbane, Qld 4001, Australia

Received 19 October 2003; received in revised form 5 April 2004; accepted 6 April 2004
Available online 24 May 2004

Abstract

A combination of high resolution thermogravimetric analysis coupled to a gas evolution mass spectrometer combined with infrared emission spectroscopy has been used to study the thermal decomposition of synthetic hydrotalcites honessite ($Ni_6Fe_2(SO_4)(OH)_{16}·4H_2O$) and mountkeithite ($Mg_6Fe_2(SO_4)(OH)_{16}·4H_2O$) and the cationic mixtures of the two minerals. High resolution thermal analysis shows the decomposition takes place in five steps. A mass loss step is observed over the 125–150 °C temperature range and is attributed to the mass loss due to dehydration. A second mass loss step is observed over the 260–330 °C temperature range and is attributed to dehydroxylation. The third mass loss occurs from 350 to 460 °C, and is assigned to a loss of oxygen. The fourth mass loss step is ascribed to the loss of sulphate from the hydrotalcite and occurs over the 676–820 °C temperature range. A mechanism for the thermal decomposition is proposed based upon the loss of water, hydroxyl units, oxygen and sulphur dioxide. The changes in the chemical structures are readily followed by infrared emission spectroscopy.

Keywords: Dehydration; Dehydroxylation; Hydrotalcite; Honessite; Mountkeithite; High-resolution thermogravimetric analysis

1. Introduction

Interest in the study of hydrotalcites results from their potential use as catalysts, adsorbents and anion exchangers [1–5]. The reason for the potential application of hydrotalcites as catalysts rests with the ability to make mixed metal oxides at the atomic level, rather than at a particle level. Such mixed metal oxides are formed through the thermal decomposition of the hydrotalcite [6,7]. Hydrotalcites may also be used as a components in new nano-materials such as nano-composites [8]. Incorporation of low levels of hydrotalcite into polymers enables polymeric materials with new and novel properties to be manufactured. There are many other uses of hydrotalcites. Hydrotalcites are important in the removal of environmental hazards in acid mine drainage [9,10]. Hydrotalcite formation also offer a mechanism for the disposal of radioactive wastes [11]. Hydrotalcite formation may also serve as a means of heavy metal removal from contaminated waters [12]. Recently, Frost et al. showed the thermal analysis patterns of several natural hydrotalcites namely carrboydite and hydrohonessite obtained from mineral deposits in Western Australia. These hydrotalcites are readily synthesised by a co-precipitation method [13–15]. In order to understand the complex relationships between iowaite/pyroaurite, stichite/woodallite and hydrotalcite/mountkeithite series, it is necessary to synthesise the minerals and determine the characteristics of the pure phase minerals.

Hydrotalcites, or layered double hydroxides (LDH) are fundamentally anionic clays [16,17]. The structure of honessite and mountkeithite can be derived from a brucite structure ($Mg(OH)_2$) in which e.g. Fe^{3+} substitutes a part of the Mg^{2+}. This substitution creates a positive layer charge on the hydroxide layers, which is compensated by interlayer anions or anionic complexes [18,19]. In hydrotalcites a broad range of compositions are possible of the type

* Corresponding author. Tel.: +61-7-3864-2407; fax: +61-7-3864-1804.
E-mail address: r.frost@qut.edu.au (R.L. Frost).

0040-6031/$ – see front matter © 2004 Elsevier B.V. All rights reserved.
doi:10.1016/j.tca.2004.04.008

$[M_{1-x}^{2+}M_x^{3+}(OH)_2][A^{n-}]_{x/n}\cdot yH_2O$, where M^{2+} and M^{3+} are the di- and trivalent cations in the octahedral positions within the hydroxide layers with x normally between 0.17 and 0.33. A^{n-} is an exchangeable interlayer anion [20]. In the hydrotalcites hydrohonessite and mountkeithite, the divalent cations are Ni^{2+} and Mg^{2+} respectively with the trivalent cation being Fe^{3+}. There exists in nature a significant number of hydrotalcites which are formed as deposits from ground water containing Ni^{2+} and Fe^{3+} [21]. These are based upon the dissolution of Ni-Fe sulphides during weathering. Among these naturally occurring hydrotalcites are mountkeithite and hydrohonessite [22,23]. Related to honessite is the mineral mountkeithite in which all or part there of, the Ni^{2+} is replaced by Mg^{2+}. These hydrotalcites are based upon the incorporation of sulphate into the interlayer with expansions of 10.34–10.8 Å.

The use of thermal analysis techniques for the study of the thermal decomposition of hydrotalcites is not common [24]. Heating sjoegrenite or pyroaurite at $<200\,^{\circ}C$ caused the reversible loss of H_2O. At 200–250 °C on static heating, or 200–350 °C on dynamic heating, very little H_2O or CO_2 were lost, but changes in the infrared spectrum and DTA effects were observed [24]. To date the number of thermal analysis studies of these minerals is very limited. Recent thermal analysis studies of the natural minerals were complicated by the formation of mixed anionic species; i.e. a mixture of hydrohonessite and mountkeithite was formed. In this work, we have synthesised these minerals and now report the thermal analysis of synthetic honessite and mountkeithite.

2. Experimental

2.1. Synthetic minerals

Minerals were synthesised by the co-precipitation method. Hydrotalcites with a composition of $(Ni,Mg)_6Fe_2(OH)_{16}(SO_4)\cdot 4H_2O$ were synthesised in an air-tight reaction vessel under nitrogen. The purpose of the reaction vessel was to eliminate the possibility of incorporation of carbonate into the hydrotalcite. Two solutions were prepared, solution 1 contained 2 M NaOH and 0.125 M Na_2SO_4, solution 2 contained 0.75 M Ni^{2+} ($Ni(NO_3)_2\cdot 6H_2O$) and 0.75 M Mg^{2+} ($Mg(NO_3)_2\cdot 6H_2O$) in the appropriate ratio, together with 0.25 M Fe^{3+} (as ($Fe(NO_3)_3\cdot 9H_2O$)). Solution 2 in the appropriate ratio was added to solution 1 using a peristaltic pump at a rate of 40 cm^3/min, under vigorous stirring, maintaining a pH of 10. The precipitated minerals are washed at ambient temperatures thoroughly with water to remove any residual nitrate. If the solution 1 contains Ni^{2+} only then the mineral hydrohonessite is formed; if the solution contains Mg^{2+} only then mountkeithite is formed. The composition of the hydrotalcites was checked by electron probe analyses. The phase composition was checked by X-ray diffraction.

2.2. Thermal analysis

Thermal decomposition of the hydrotalcite was carried out in a TA® Instruments incorporated high-resolution thermogravimetric analyser (series Q500) in a flowing nitrogen atmosphere (80 cm^3/min). Approximately, 50mg of sample was heated in an open platinum crucible at a rate of 2.0 °C/min up to 500 °C. No preparation was required other than grinding the sample up finely. With the quasi-isothermal, -isobaric heating program of the instrument the furnace temperature was regulated precisely to provide a uniform rate of decomposition in the main decomposition stage. The TGA instrument was coupled to a Balzers (Pfeiffer) mass spectrometer for gas analysis. Only selected gases were analysed.

2.3. Infrared emission spectroscopy

FTIR emission spectroscopy was carried out on a Nicolet spectrometer equipped with a TGS detector, which was modified by replacing the IR source with an emission cell. A description of the cell and principles of the emission experiment have been published elsewhere [25–27]. Approximately, 0.2 mg of honessite or mountkeithite was spread as a thin layer (approximately 0.2μm) on a 6 mm diameter platinum surface and held in an inert atmosphere within a nitrogen-purged cell during heating. Spectral manipulation such as baseline adjustment, smoothing and normalisation was performed using the GRAMS® software package (Galactic Industries Corporation, Salem, NH, USA).

3. Results and discussion

3.1. X-ray diffraction

The X-ray diffraction patterns of the synthesised reevesite and mixed cationic honessites are shown in Fig. 1. The XRD patterns clearly show the synthetic minerals are layered structures with interspacing distances of around 9.0 Å. Some subtle variations in the d(0 0 1) spacing are observed. The honessite ($Ni_6Fe_2(SO_4)(OH)_{16}\cdot 4H_2O$) has a d(0 0 1) spacing of 9.24 Å. Upon replacement of 1 mol of Ni with Mg, the honessite ($(MgNi_5Al_2(SO_4)(OH)_{16}\cdot 4H_2O$) is formed. The d spacing decreases to 9.20 Å. Upon replacement of a second mole of Ni, the honessite ($(Mg_2Ni_6Al_2(SO_4)(OH)_{16}\cdot 4H_2O$) is formed. The d-spacing decreases to 9.13 Å. With the equimolar mixed hydrotalcite ($(Mg_3Ni_3Al_2(SO_4)(OH)_{16}\cdot 4H_2O$) the d spacing reaches 8.94 Å. Further increasing the Mg content results in an expansion of the interlayer space to 9.23 Å. Previous studies have shown that the natural minerals have an interlayer space of 10.8 Å [28–30]. The effect of cation replacement of Ni by Mg causes a decrease in the interlayer spacing. Previous studies have suggested that only the size of the anion effected the interlayer space [27]. The reason for

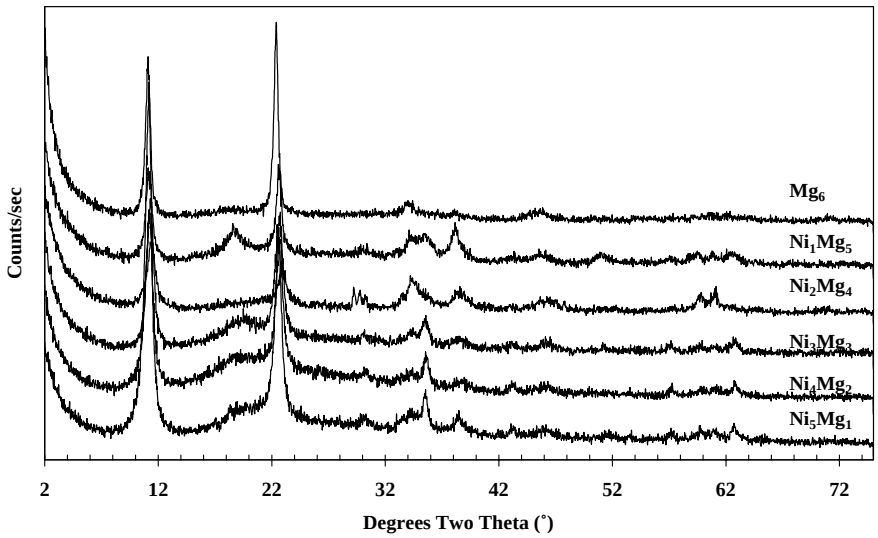

Fig. 1. X-ray diffraction pattern of honessite and mountkeithite and their cationic mixtures.

this change in interlayer space may be attributed to the difference in cation size between the Mg^{2+} and the Ni^{2+}. The end-members of honessite and mountkeithite have the largest interlayer spacing. A previous study of synthetic hydrohonessite also showed the interlayer space was ~9.0 Å [30]. However honessite has a spacing of around 9.0 Å, so it is likely that the series honessite–mountkeithite rather than hydrohonessite–mountkeithite has been synthesised in this work.

3.2. High resolution thermogravimetric analysis and mass spectrometric analysis

The high resolution thermogravimetric analysis (HRTG) for the synthetic honessite–mountkeithite series are shown in Fig. 2. The evolved gas mass spectrometric curves are shown in Fig. 3. The results of the analyses of the mass loss and temperature of the mass loss are reported in Table 1. The temperatures of the evolved gas MS mass gain are reported in Table 2. Several mass loss steps are observed. A mass loss step is observed over the 125–150 °C temperature range and is attributed to the mass loss due to dehydration. A second mass loss step is observed over the 260–330 °C temperature range and is attributed to dehydroxylation. The third mass loss occurs from 350 to 460 °C, and is assigned to a loss of oxygen. The fourth mass loss step is ascribed to the loss of sulphate from the hydrotalcite and occurs over the 676–820 °C temperature range. A second dehydroxylation step is observed for some of the hydrotalcites. The mass loss step for the loss of sulphate occurs over a wide temperature range. The % mass loss for dehydration varies from 7.3% up to 8%. This mass loss may be compared with a theoretical mass loss of 7.96 for Ni_6 to 10.34 for Mg_6. The experimental % mass loss during dehydroxylation varies from 14.5% up to 24.6%. The theoretical mass loss for dehydroxylation varies from 15.9 to 20.6%. The experimental % mass loss during de-oxygenation varied from 2.82 to 3.83%. The theoretical % loss for this loss was from 3.54 to 4.59%. There was a small amount of variation in these results. This could be due to differences in the actual amount of oxygen lost. The temperatures for the loss of sulphate vary from 676 to 820 °C.

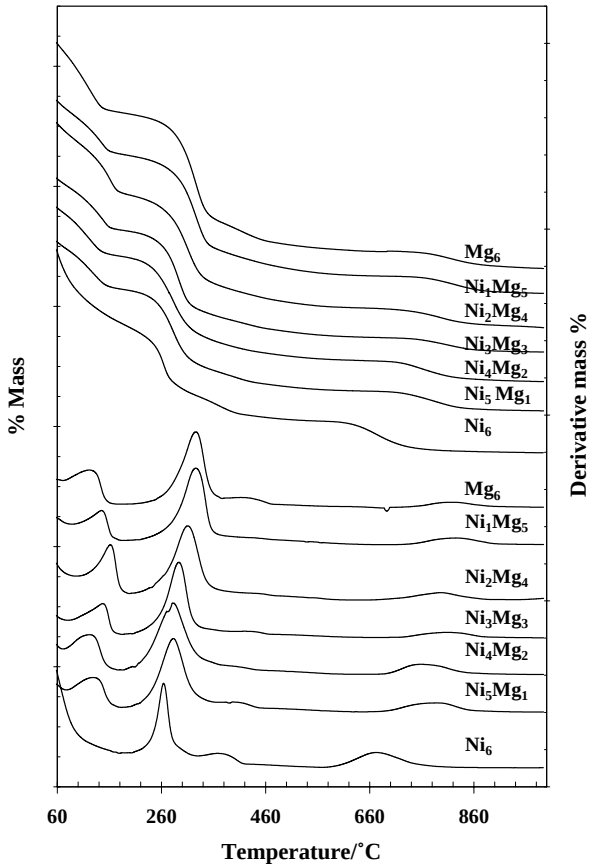

Fig. 2. High resolution thermogravimetric analyses of honessite and mountkeithite and their cationic mixtures.

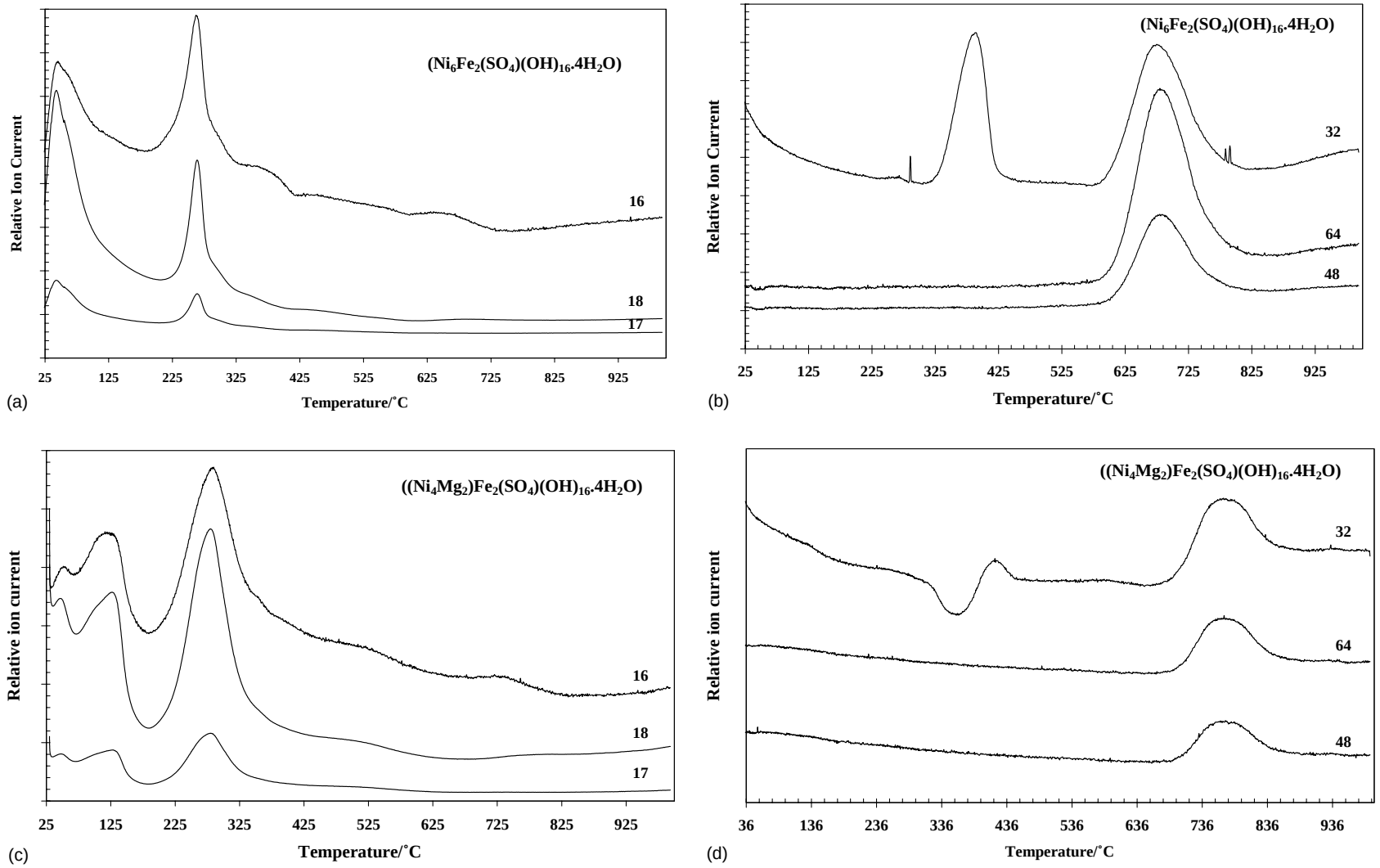

Fig. 3. Mass spectrometric curves for honessite and mountkeithite and their cationic mixtures.

Table 1
Results of the HRTG of synthetic honessite–mountkeithite

Honessite–mountkeithite	Dehydration			Dehydroxylation			De-oxygenation			De-sulphation		
	% Mass loss, step1	Theoretical % mass loss	Temperature	% Mass loss, step 2	Theoretical % mass loss	Temperature	% Mass loss, step 3	Theoretical % mass loss	Temperature	% Mass loss, step 4	Theoretical % mass loss	Temperature
Ni_6	9.5	7.96	133	16.37	15.93	268	5.55	3.54	379	6.33	7.08	676
Ni_5Mg	7.5	8.28	135	16.6	16.56	285	3.43	3.68	400	3.83	7.36	786
Ni_4Mg_2	8.97	8.62	125	14.5	17.24	284	5.17	3.83	353	3.45	7.66	770
Ni_3Mg_3	8.51	9.00	150	19.12	17.98	295	5.87	4.00	416	2.53	7.99	811
Ni_2Mg_4	9.20	9.40	163	20.74	18.79	313	3.13	4.18	428	3.63	8.35	803
$NiMg_5$	7.38	9.84	148	22.01	19.67	328	3.49	4.37	460	3.23	8.74	831
Mg_6	8.06	10.32	125	24.62	20.64	329	5.15	4.59	421	2.82	9.17	820

Table 2
Results of the evolved gas mass spectrometry of synthetic honessite–mountkeithite

Honessite–mountkeithite	Temperature			
	Dehydration	Dehydroxylation	De-oxygenation	Desulphation
Ni_6	140	265	390	683
Ni_5Mg	136	284	410	803
Ni_4Mg_2	130	283	414	777
Ni_3Mg_3	150	294	443	823
Ni_2Mg_4	165	307	456	777
$NiMg_5$	147	324	502	800
Mg_6	131	322	446	830

There was a considerable difference between theoretical and actual loss of sulphate. This may be due to some sulphates being bound more strongly to the hydrotalcite lattice. One possibility is that after the dehydration and dehydroxylation steps the metal oxide surfaces are highly surface energetic. Therefore, the sulphate reacts with the oxides to form sulphates. Further, not all sulphate may be taken up in the hydrotalcite formation; some amorphous iron phases may have formed. The XRD patterns show some background in the 22° 2θ indicating some amorphicity. It was observed that after heating, the samples were no longer finely ground, but rather fused together in a solid mass. Because of this, there may have been some sulphates embedded in the mass which could not evolve as a gas within the temperature range of the experiment. Fig. 2 shows certain trends in the mass loss steps: (a) the temperature of dehydration increases with increased substitution. The temperature increases for Mg_3Ni_3 and then decreases. (b) The temperature of dehydroxylation increases as the Mg content is increased. (c) The temperature for the loss of sulphate increases with Mg content.

The mass spectrometric results of the evolved gases are shown in Fig. 3. The MS of evolved water vapour clearly shows dehydration occurring in three steps. The first mass gain occurs at low temperatures (Table 2). The temperatures vary between 46 and 60 °C. The second mass gain occurs in the temperature range 130–165 °C. This temperature appears to be a function of the composition of the hydrotalcite and increases with increasing substitution. The temperature of this second mass gain of evolved water vapour is in excellent agreement with the values determined by HRTG. In the MS curves for O = 16, evolved gas of oxygen occurs over the 390–456 °C temperature range. The temperature appears to be composition dependent and increases with Mg content. This evolved gas appears to coincide with a small mass loss step observed at around the 400 °C temperature range in the HRTG steps. Fig. 3 shows the mass spectra for S or O_2 (32), SO_2 or S_2 (64) and SO (48). The temperatures for the loss of sulphate as SO_2 are reported in Table 2. Some variation in the temperature for the loss of SO_2 is observed. The temperatures vary between 683 (Ni_6) and 830 (Mg_6). The values are in good agreement with the results of HRTG.

Mechanism for the thermal decomposition of honessite–mountkeithite series

For the decomposition of natural hydrohonessite six decomposition steps were observed. The problem with using the natural sample is that a mixture of interlayer anions complicates the thermal decomposition. In the case of the natural hydrohonessite, both sulphate and carbonate anions were found in the interlayer. For the synthetic honessite, this difficulty is removed. For the natural honessite, three weight loss steps were observed at 71, 95.6 and 137 °C and are attributed to dehydration. Two weight loss steps were observed for natural honessite at 294 and 329 °C with a total weight loss of 10.5% attributed to dehydroxylation. The weight loss step is observed at 646 °C, and is attributed to loss of sulphate. This temperature is less than that observed for the synthetic honessites. The results for the synthetic honessite correspond well with those for the natural honessite. In the study of natural honessite, it was not obvious that oxygen was one of the evolved gases; whereas for the synthetic honessites, oxygen is evolved in the 390–456 °C temperature range.

3.3. Infrared emission spectroscopy

The thermal decomposition of the synthetic hydrotalcites can be monitored using vibrational spectroscopy and a thermal stage. One technique of doing this is by infrared emission spectroscopy. The infrared emission spectra of the hydroxyl stretching region of selected honessite and mountkeithite cationic mixtures are shown in Fig. 4. The spectra at 100 °C show a low signal to noise ratio due to low thermal emission energy. The spectra for Mg_6 and Ni_2Mg_4 cationic mixtures show a series of peaks between 2980 and 2850 cm^{-1} which are caused by adsorbed isopropanol. Isopropanol was used to suspend the sample to give an even distribution of sample for IR spectroscopic analysis. There was no isopropanol required for the other two samples.

Fig. 4 clearly shows the loss of both water and hydroxyls as thermal decomposition of the hydrotalcite takes place. The Mg_6 hydrotalcite (at 300 °C) shows four curve resolved bands at 3677, 3606, 3512 and 3374 cm^{-1}. At 400 °C, only two bands are observed at 3610 and 3494 cm^{-1}. At 600 °C no intensity remains. One probable assignment is that the first two bands are assignable to OH stretching vibrations from MgOH and AlOH units and the last two bands to water OH stretching bands. For the Ni_6 hydrotalcite, at 300 °C, bands are observed at 3656, 3559 and 3441 cm^{-1} (Fig. 4d). The first band is attributed to the NiOH stretching vibration; the other two bands are due to water OH stretching vibrations. As Mg is introduced into the Ni_6 hydrotalcite in-

Step 1. Low temperatures: $(Ni_{(6-x)}Mg_x)\ Fe_2(SO_4)(OH)_{16}{\cdot}4H_2O \rightarrow (Ni_{(6-x)}Mg_x)\ Fe_2(SO_4)(OH)_{16} + 4H_2O$
Step 2. Temperature range 130–160 °C: $(Ni_{(6-x)}Mg_x)\ Fe_2(SO_4)(OH)_{16} \rightarrow (Ni_{(6-x)}Mg_x)O_{y/2}\ Fe_2(SO_4)(OH)_{16-y} + y/2H_2O$
Step 3. Temperature range 268–329 °C: $(Ni_{(6-x)}Mg_x)O_{y/2}\ Fe_2(SO_4)(OH)_{16-y} \rightarrow (Ni_{(6-x)}Mg_x)O_8\ Fe_2(SO_4)+(16-y)/2H_2O$
Step 4. Temperature range 390–456 °C: $(Ni_{(6-x)}Mg_x)O_8\ Fe_2(SO_4) \rightarrow (Ni_{(6-x)}Mg_x)O_7\ Fe_2(SO_3) + O_2$
Step 5. Temperature range 680–830 °C: $(Ni_{(6-x)}Mg_x)O_7\ Fe_2(SO_3) \rightarrow (Ni_{(6-x)}Mg_x)O_5\ Fe_2O_3 + (SO_2)$

The five steps listed above show the chemical reactions and the appropriate temperature range for the thermal decomposition. The reactions show that in order to make a mixed metal oxide based upon Ni, Mg and Fe, a temperature of 800 °C must be reached.

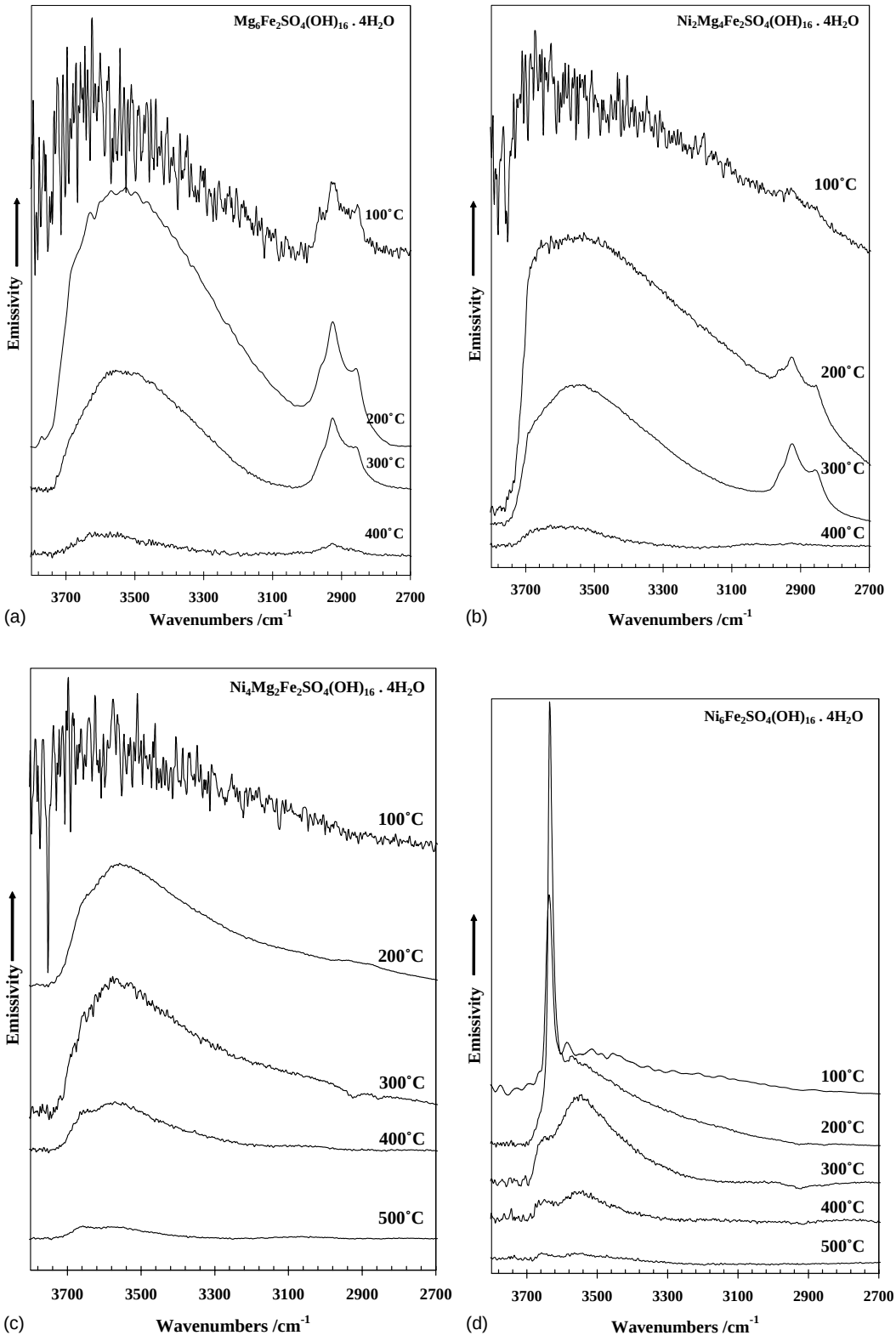

Fig. 4. Infrared emission spectra of the hydroxyl stretching region of honessite and mountkeithite and their cationic mixtures.

creased complexity is observed in the OH stretching region. For the Ni_4Mg_2 hydrotalcite (at 300 °C) bands are observed at 3665, 3602, 3522, 3393 and 3189 cm^{-1} (Fig. 4c).

4. Conclusions

The HRTGA of the two related minerals honessite and mountkeithite have been studied. These hydrotalcite minerals show at least five mass loss steps ascribed to (a) water-desorption, (b) dehydration, (c) dehydroxylation, (d) loss of oxygen and (e) de-sulphating. (a) HRTG shows that the temperature of dehydration increases with increased substitution. The temperature increases for Mg_3Ni_3 and then decreases. (b) The temperature of dehydroxylation increases as the Mg content is increased. (c) The temperature for the loss of sulphate increases with Mg content. Mechanisms for the thermal decomposition of the honessite–mountkeithite series are proposed. The effect of cation substitution reduces the interlayer distance.

Infrared emission spectroscopy shows the changes in the molecular structure of the hydrotalcites as thermal decomposition takes place. IES of the hydroxyl stretching region shows the temperatures at which no intensity remains in the OH stretching vibrations. These temperatures are in good agreement with the results of the thermal analysis.

References

[1] J. Theo Kloprogge, R.L. Frost, Appl. Catal. A: Gen. 184 (1999) 61.
[2] A. Alejandre, F. Medina, X. Rodriguez, P. Salagre, Y. Cesteros, J.E. Sueiras, Appl. Catal. B 30 (2001) 195.
[3] J. Das, K. Parida, React. Kinet. Catal. Lett. 69 (2000) 223.
[4] S.H. Patel, M. Xanthos, J. Grenci, P.B. Klepak, J. Vinyl Addit. Technol. 1 (1995) 201.
[5] V. Rives, F.M. Labajos, R. Trujillano, E. Romeo, C. Royo, A. Monzon, Appl. Clay Sci. 13 (1998) 363.
[6] F. Rey, V. Fornes, J.M. Rojo, J. Chem. Soc., Faraday Trans. 88 (1992) 2233.
[7] M. Valcheva-Traykova, N. Davidova, A. Weiss, J. Mater. Sci. 28 (1993) 2157.
[8] C.O. Oriakhi, I.V. Farr, M.M. Lerner, Clays Clay Miner. 45 (1997) 194.
[9] G. Lichti, J. Mulcahy, Chem. Aust. 65 (1998) 10.
[10] Y. Seida, Y. Nakano, J. Chem. Eng. Jpn. 34 (2001) 906.
[11] Y. Roh, S.Y. Lee, M.P. Elless, J.E. Foss, Clays Clay Miner. 48 (2000) 266.
[12] Y. Seida, Y. Nakano, Y. Nakamura, Water Res. 35 (2001) 2341.
[13] M.A. Aramendia, V. Borau, C. Jimenez, J.M. Marinas, J.M. Luque, J.R. Ruiz, F.J. Urbano, Mater. Lett. 43 (2000) 118.
[14] V.R.L. Constantino, T.J. Pinnavaia, Inorg. Chem. 34 (1995) 883.
[15] M. Del Arco, P. Malet, R. Trujillano, V. Rives, Chem. Mater. 11 (1999) 624.
[16] K. Hashi, S. Kikkawa, M. Koizumi, Clays Clay Miner. 31 (1983) 152.
[17] L. Ingram, H.F.W. Taylor, Mineral. Mag. J. Mineral. Soc. (1876–1968) 36 (1967) 465.
[18] R.M. Taylor, Clay Miner. 17 (1982) 369.
[19] H.F.W. Taylor, Mineral. Mag. J. Mineral. Soc. (1876–1968) 37 (1969) 338.
[20] H.C.B. Hansen, C.B. Koch, Appl. Clay Sci. 10 (1995) 5.
[21] E.H. Nickel, J.E. Wildman, Mineral. Mag. 44 (1981) 333.
[22] D.L. Bish, A. Livingstone, Mineral. Mag. 44 (1981) 339.
[23] E.H. Nickel, R.M. Clarke, Am. Mineral. 61 (1976) 366.
[24] P.G. Rouxhet, H.F.W. Taylor, Chimia 23 (1969) 480.
[25] L. Hickey, J.T. Kloprogge, R.L. Frost, J. Mater. Sci. 35 (2000) 4347.
[26] J.T. Kloprogge, L. Hickey, R.L. Frost, Appl. Clay Sci. 18 (2001) 37.
[27] J.T. Kloprogge, D. Wharton, L. Hickey, R.L. Frost, Am. Mineral. 87 (2002) 623.
[28] D.L. Bish, A. Livingstone, Mineral. Mag. 44 (1981) 339.
[29] D.L. Bish, G.W. Brindley, Am. Mineral. 62 (1977) 458.
[30] E.H. Nickel, J.E. Wildman, Mineral. Mag. 44 (1981) 333.